

Original Article

Reactivation of oncogenes involved in G1/S transcription and apoptosis pathways by low dose decitabine promotes HT29 human colon cancer cell growth in vitro

Xiaojie Wang, Pan Chi

Department of Colorectal Surgery, Union Hospital, Fujian Medical University, People's Republic of China

Received July 13, 2020; Accepted October 1, 2020; Epub December 15, 2020; Published December 30, 2020

Abstract: Background: To examine the effects of low-dose decitabine (DAC) on the proliferation of HT-29 cell lines, and to explore the central mechanism by which low-dose DAC affects HT-29 cell proliferation using a systematic biological approach. Methods: First, we examined the global effects of DAC on cell proliferation, the cell cycle, and apoptosis in HT29 colon cancer cells. Then, a series test of cluster (STC) analysis and weighted gene coexpression network analysis (WGCNA) were employed to identify critical pathways involved in the response to DAC treatment using 3 datasets from the GEO database. Finally, the expression changes and promoter methylation levels of hub genes were further confirmed by in vitro experiments. Results: Low-dose DAC (less than 1 μ M) promoted the proliferation and colony formation ability of HT-29 cell lines. The results of the system-level analysis, including STC analysis, WGCNA, and Gene set variation analysis (GSVA), showed that DAC modulated 3 critical pathways: G1/S-specific transcription involved in E2F-mediated regulation of Cyclin E-associated events, apoptosis pathways, and EMT pathways. Subsequent in vitro experiments showed that low-dose DAC (0.1 μ M) promoted G1/S-specific transcription and decreased apoptosis rates. Then, several regulatory hub oncogenes in these 3 pathways, CCNE1, E2F1, BCL2, PCNA, FOXC1, VIM, CXCL1, and VCAM1, were further confirmed to be activated by DAC at either the mRNA or protein level. We chose the oncogene BCL2 as an example and detected its methylation status and the effect of low-dose DAC on BCL2 expression. Data from TCGA and Oncomine databases demonstrated that BCL2 was decreased in colon cancer compared with normal mucosa. Further analysis showed that BCL2 had an increased degree of promoter methylation in 12 methylated sites in colon cancer compared with normal colon tissues. Bisulfite sequencing PCR showed that low-dose DAC decreased the methylation rate at the BCL2 promoter region. Conclusions: We concluded that low-dose DAC treatment resulted in a cancer-promoting effect in HT29 cell lines. Mechanistically, high methylation levels at the promoter region of oncogenes with dominant effects in CRC, such as BCL2 in HT29, might play a role in suppressing CRC by inhibiting oncogene expression. Low-dose DAC treatment triggered BCL2 expression by decreasing its promoter methylation level, thereby resulting in cancer promotion.

Keywords: Decitabine, colon cancer, DNA methylation

Introduction

Colorectal cancer (CRC) is one of the major malignancies worldwide and an important cause of health care costs [1]. Furthermore, nearly 50% of CRC patients are either diagnosed at a late stage at the first visit, or they develop distant metastases during treatment or follow-up, which makes CRC one of the most common cancer-related mortalities [2]. It is known that methylation in the promoter regions of genes can turn off their tumor suppressing

potential [3]. One important part of epigenetics is regulated by DNA methyltransferases (DNMTs). Under the catalysis of DNMTs, a methyl group is covalently added to a cytosine in a CpG dinucleotide, which changes chromatin structure and leads to gene silencing [4]. 5-Aza-29-deoxycytidine (decitabine, DAC) is one of the most popular DNMT inhibitors, and it can reverse epigenetic changes resulting in reactivation of inhibited suppressor genes, decreasing tumorigenesis [5]. Epigenetic drugs have shown beneficial effects for hematological

malignancies, which has led to the approval of DAC by the FDA for treating all subtypes of myelodysplastic syndromes and low-blast count acute myeloid leukemia [6]. However, clinical trials assessing the use of DNMT inhibitors in solid tumors, including CRC, regardless of their molecular features, failed to improve the overall oncological outcomes [5].

The development of CRC proceeds through the acquisition of genetic aberrations during cancer progression [7]. The alterations in genomic expression might be caused by epigenetic aberrations [8], mutations [9], or copy number variation [10]. However, the regulatory mechanism through which the hub gene is regulated in different individuals with CRC is still unknown. Moreover, due to the different key molecular features involved in different CRC cell types, the mechanism through which anticancer drugs function in different CRC cell types has yet to be revealed [11]. A previous study showed that human HCT116 CRC cells exhibited the highest sensitivity to DAC, while HT29 CRC cells exhibited the highest resistance among four human CRC cell lines (HT29, SW480, SW48 and HCT116) [12]. The difference in IC_{50} values between HT29 and HCT116 cells was approximately 824-fold [12]. In another study, DAC showed an inhibitory effect at a starting concentration of 20 μ M in HT-29 CRC cells, but this concentration is intolerable to humans [13]. The concentration of DAC required to inhibit DNA methylation in clinical applications was reported to be \sim 0.3 μ M, which is the maximal tolerable plasma concentration in Humans [14]. The effect of low-dose DAC (less than 1 μ M) on the proliferation of HT-29 cell lines is still unknown.

In the present study, we first examined the effects of low-dose DAC, which can effectively inhibit DNMT, on the proliferation of HT-29 cell lines. Since hypermethylated genes can be reactivated after DAC treatment, mapping these genes onto a network may elucidate the key pathways activated after low-dose DAC treatment. Series test of cluster (STC) analysis and weighted gene coexpression network analysis (WGCNA) can expose the system-level functionality of a transcriptome to identify network-centric genes associated with drug treatment [15, 16]. Therefore, we utilized these two bioinformatic approaches to evaluate the relationships between genes subjected to DAC

treatment and to explore and confirm the central mechanism by which low-dose DAC affects HT-29 cell proliferation.

Materials and methods

Cell culture and DAC treatment

HT-29 CRC cell lines (Shanghai Genechem Co., Ltd, Shanghai, China) were cultured in Dulbecco's modified Eagle's medium (DMEM: HyClone, USA) containing 10% fetal bovine serum (EVERY GREEN FBS: TIANHANG, Zhejiang, China) and 1% streptomycin-penicillin, and they were maintained in a 37°C, 5% CO₂ incubator.

DAC (Qilu Pharmaceutical Co., Ltd, Shandong, China) was dissolved in PBS. The concentrations of DAC ranged from 10⁻³ to 100 μ M based on its pharmacological dose and on our preliminary experiments. Cells were incubated with DAC for 48 h.

Cell counting kit-8 (CCK-8) assay

Cells were first seeded into 96-well plates at a density of 5×10³ cells per well. At the appointed time points, 110 μ L of fresh medium containing 10 μ L of CCK-8 solution (Beyotime, Shanghai, China) was added, and then the cells were incubated for 1 h in the dark. Absorbance values at 450 nm were measured using a microplate reader.

Colony formation assays

Cells were plated at a density of 800 cells per well in 6-well plates and cultured for 24 h and then DAC was added. After 10 to 14 days, the colonies were stained with 0.2% crystal violet with buffered formalin (Beyotime, Shanghai, China). Colony numbers were counted using ImageJ (NIH, Bethesda, USA).

Datasets

A total of three microarray datasets were obtained from the Gene Expression Omnibus (GEO) database. GSE41364 [17] contained mRNA expression profiles from HT-29 colon cancer cell lines treated with 3 concentrations of 5-aza-deoxy-cytidine (0 μ M, 5 μ M, and 10 μ M) for 5 days. GSE32323 [18] contained 2 mRNA expression profiles from HT-29 cell lines before and after 5-aza-2'-deoxycytidine treat-

ment. GSE22598 [19] contained another 2 mRNA expression profiles of HT-29 cell lines before and after DAC treatment at 0.5 μ M for 72 h. The microarray quality was measured by sample clustering. Related gene expression was subjected to identical processing using the Robust Multichip Average function within the limma R package. The mean value was used if multiple probes were mapped to a gene symbol. The missing values were filled using the Impute R package.

The expression and methylation data of a DAC-activated gene, BCL-2, in CRC from The Cancer Genome Atlas (TCGA) database were obtained from MEXPRESS [20]. Oncomine (<https://www.oncomine.org>) was used to confirm the differential expression levels of BCL2 between CRC and normal tissues [21].

STC

STC analysis was performed to study the changes in gene expression and to determine different expression tendencies as a result of increasing concentrations of drug treatment. These genes with the same expression change trends were clustered for further analysis.

WGCNA

The data from GSE41364 were used to construct scale-free coexpression networks using the WGCNA algorithm as previously reported [16]. The correlation between genes was evaluated by a Pearson correlation matrix and the connecting rod means. The soft thresholding power was calculated by network topology analysis, and the adjacency was converted to the topological overlap matrix (TOM) [22]. Average linkage hierarchical clustering was performed basing the TOM-based dissimilarity measure to cluster genes into modules [23]. The hub modules subject to DAC treatment were identified by Pearson's correlation analysis.

Functional enrichment analysis

FunRich was used on the most representative trend profile from the STC analysis and hub modules from the WGCNA to identify hub pathways involved in DAC treatment using a community-driven approach [24]. Gene set variation analysis (GSVA) was used to estimate the pathway activity changes over a sample population subject to DAC treatment in an unsupervised manner [25].

Cell cycle determination

Cells were digested and fixed in precooled 70% ethanol at 4°C overnight, and then they were incubated with 10 μ L of RNase A (50 \times) before being dyed with propidium iodide (KeyBEN BioTECH, Jiangsu, China) for 30 min. The volume was then increased to 535 μ L, and the cells were analyzed using a FACSCalibur flow cytometer (BD Biosciences).

Apoptosis quantitation

Apoptosis detection was performed by double staining using an Annexin V-PE/7-AAD Apoptosis Detection kit (KeyGEN BioTECH, Jiangsu, China). Cells were collected and washed with PBS. Then, 5 μ L of 7-AAD was added and incubated with the cells for 5 min, which was followed by the addition of 1 μ L of annexin V and incubation for 15 min in the dark before flow cytometry analysis.

Hub gene verification by bioinformatic analysis

Two datasets (GSE32323 and GSE22598) were used to verify the mRNA expression of VIM, CXCL1, VCAM1, E2F3, E2F1, CCNE, PCNA, FOXC1, and BCL2 between the DAC treatment group and the control group.

Hub gene verification by real-time quantitative polymerase chain reaction (RT-qPCR)

Total RNA was isolated using TRIzol reagent (Thermo Fisher Scientific, USA), and 1 μ g of total RNA was used for reverse transcription reaction using Reverse Transcriptase Product (Thermo Scientific Revert Aid, USA) under the following conditions: 42°C for 60 min, 70°C for 5 min, and storage at -80°C. RT-qPCR was performed using an ABI 7500 real-time PCR system (Thermo Fisher Scientific, USA) under the following conditions: 95°C for a 10 min initial denaturation step, followed by 95°C for 15 s, and annealing and extension at 60°C for 60 s for 40 cycles. Gene-specific intron-spanning primers are shown in **Table 1**. The relative expression of mRNA was calculated using the $\Delta\Delta$ Cq method, and GAPDH was used as an internal control.

Western blot analysis

Total protein was extracted from cells by incubating them with radioimmunoprecipitation assay (RIPA) containing phenylmethanesulfonyl

Table 1. PCR Primers

	Forward (5'-3')	Reverse (5'-3')
IVCAM1	TTTGACAGGCTGGAGATAGACT	TCAATGTGTAATTTAGCTCGGCA
BCL2	GACTTCGCCGAGATGTCCAG	GAACTCAAAGAAGGCCACAATC
E2F3	GCTTCAACCAACTCAGGACATAG	CCGAGGCTCAGGAGATAGTC
CCNE1	GCCAGCCTTGGGACAATAATG	CTTGACGTTGAGTTTGGGT
GAPDH	AGAAGGCTGGGGCTCATTTG	AGGGGCCATCCACAGTCTTC
VIM	AGTCCACTGAGTACCGGAGAC	CATTTACGCATCTGGCGTTC
PCNA	CCTGCTGGGATATTAGCTCCA	CAGCGGTAGGTGTGCAAGC
CXCL1	GGAATTCACCCCAAGAACATC	GGATGCAGGATTGAGGCAAGC
FOXC1	TGTTTCGAGTCACAGAGGATCG	ACAGTCGTAGACGAAAGCTCC
E2F1	CATCCCAGGAGGTCACTTCTG	GACAACAGCGTTCTTGCTC

fluoride (PMSF) (Beyotime, Shanghai, China) on ice for 30 min. Protein concentrations were measured using a BCA Protein Assay kit (Beyotime, Shanghai, China). Protein samples were separated by electrophoresis and then were transferred onto polyvinylidene difluoride (PVDF) membranes. After blocking with 5% nonfat milk for 1.5 h, the membranes were incubated at 4°C overnight with human antibodies specific to Cyclin E1, PCNA, Bax, Bcl-2 and GAPDH (Bioss Antibodies, Beijing, China). Then, the membranes were incubated with an IgG/HRP antibody (Bioss Antibodies, Beijing, China) for 1.5 h; finally, the membranes were visualized using an enhanced chemiluminescence (ECL) method and were analyzed by ImageJ.

Bisulfite sequencing PCR

Genomic DNA was isolated using a TIANamp Genomic DNA kit (TIANGEN Biotech, Beijing, China), and the bisulfite modification process was performed (TSINGKE Biotech, Beijing, China). The primers were 5'-GATTTTGTTTTATAGAAATGTTAAT-3' (forward) and 5'-CTCTCCCCTATCTCTCTCTAAA-3' (reverse). The PCR conditions were as follows: denaturation at 98°C for 2 min, 30 cycles at 98°C for 10 s, 55°C for 30 s, and 72°C for 30 s. PCR products were purified using a TIAN gel Midi Purification kit (TIANGEN Biotech, Beijing, China) and used to transform competent cells. Isolated positive clones on LB agar plates were selected and sequenced.

Statistical analysis

Continuous variables were compared using Student's t-test. Statistical analyses were conducted using GraphPad Prism 7 and R (ver.

3.5.1) or SPSS version 20.0 (SPSS, Inc., Chicago, IL, USA). A *P*-value < 0.05 was considered to indicate statistical significance.

Results

Low-dose DAC accelerated HT-29 proliferation

CCK-8 assays indicated that DAC, used in the concentration range from 10⁻³ to 0.1 μM, promoted the proliferation of HT-29 cells in vitro, while it showed no effect on survival in the concentration

range from 1 to 10 μM; further, it showed an inhibitory effect at concentrations greater than 10 μM (**Figure 1A, 1B**). Similarly, low-dose DAC (0.1 μM) treatment significantly increased the colony formation ability of HT-29 cells in vitro and slightly decreased the colony formation ability at a concentration of 1 μM (**Figure 1C**). As presented in **Figure 1D, 1E**, HT-29 cells exhibited a cobblestone shape. Interestingly, following 0.1 μM DAC treatment for 48 h, HT-29 cells exhibited a spindle shape with mesenchymal morphology.

STC analysis and WGCNA

To explore the mechanism by which low-dose DAC treatment promoted proliferation, WGCNA and STC analyses were performed. In WGCNA, the thresholding power of β = 5 was chosen to construct a scale-free network (**Figure 2A**). The coexpression analysis identified a total of 103 modules (**Figure 2B**). Among them, a total of 6 modules correlated with DAC treatment and were included in further analysis (**Figure 2C**). STC analysis identified 3 profiles that included genes with similar expression trends as a result of DAC treatment. The expression trend of genes in these 3 profiles generally showed a trend toward concentration-dependent increase after DAC treatment. Of the profiles, profile 6 (*P* = 3.7E-169, **Figure 2D, 2E**) exhibited the highest significance and was selected for further pathway enrichment analysis. In profile 6, a total of 2893 genes showed an upward trend in expression during zero- to low-dose DAC treatment, with no expression change during low- to high-dose DAC treatment.

Pathway enrichment analysis of significant profiles in STC analysis and hub modules in WGCNA

Low-dose decitabine treatment of HT29 colon cancer cells

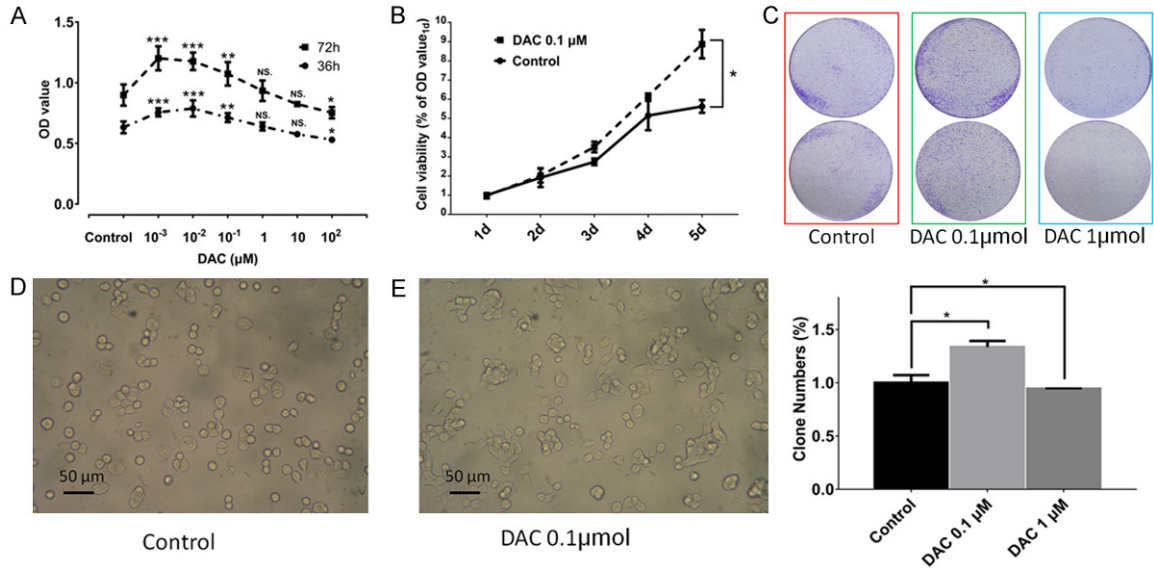


Figure 1. Low-dose DAC treatment promoted HT29 CRE cell proliferation. A. CCK-8 assays were performed. Low-dose DAC in the concentration range from 10^{-3} to $0.1 \mu\text{M}$ promoted the proliferation of HT-29 cells in vitro, while DAC showed no effect on proliferation in the concentration range from 1 to $10 \mu\text{M}$ and an inhibitory effect at concentrations greater than $10 \mu\text{M}$. B. DAC at $0.1 \mu\text{M}$ promoted the proliferation of HT-29 cells from days one to five. C. Low-dose DAC ($0.1 \mu\text{M}$) increased colony formation ability in HT-29 cells in vitro, and it slightly decreased colony formation ability when used at a concentration of $1 \mu\text{M}$. D. Parent HT-29 cells exhibited a cobblestone shape. E. HT-29 cells exhibited a spindle shape following $0.1 \mu\text{M}$ DAC treatment.

was performed. DAC primarily modulated 3 pathways (KEGG): G1/S-specific transcription involved in E2F-mediated regulation of cyclin E-associated events, epithelial-to-mesenchymal transition (EMT) and regulation of apoptosis (Figure 2F). Among these pathways, GSVA revealed that G1/S-specific transcription was activated by low-dose DAC treatment and was inhibited by treatment with a higher dose (Figure 2G). The EMT pathway activity was slightly increased during zero- to high-dose DAC treatment, while apoptosis was consistently inhibited (Figure 2H).

Effect of low-dose DAC on cell cycle progression and apoptosis

The pathway enrichment analysis prompted us to further examine the cell cycle and apoptotic phenotypes of HT-29 cells subjected to DAC treatment. Treatment with $0.1 \mu\text{M}$ DAC resulted in an increase in the number of cells in the S phase compared to that of the control group (DAC vs control: 27.0% vs 14.7%) at the expense of the G1 phase (DAC vs control: 57.4% vs 67.6%) (Figure 3A-C). The results indicated that low-dose DAC treatment promoted G1/S-specific transcription, which was consistent

with the pathway enrichment analysis. The percentage of early apoptotic and total apoptotic cells slightly decreased by $\sim 1\%$ when cells were cocultured with low-dose DAC at concentrations ranging from 10^{-2} to $10 \mu\text{M}$ (Figure 3D-F).

Verification of hub gene expression in G1/S-specific transcription

In this study, we observed that low-dose DAC treatment promoted G1/S-specific transcription, and enrichment analysis showed that this process might be involved in E2F-mediated regulation of Cyclin E-associated events. Cyclin E1, encoded by CCNE1, promotes the activation of E2F-mediated transcription and drives cells from G1 into S phase [26]. This prompted us to further examine hub gene expression in the E2F/CCNE1 pathway in HT-29 cells subjected to DAC treatment. In both the GSE41364 dataset and the GSE32323 dataset, DAC increased E2F1 and CCNE1 expression at the mRNA level (Figure 4A, 4B). Furthermore, the results of qPCR in our in vitro experiment showed that E2F1, E2F3 and CCNE1 expression was upregulated in response to $0.1 \mu\text{M}$ DAC (Figure 4C). We also confirmed the protein expression of the G1/S-specific transcription

Low-dose decitabine treatment of HT29 colon cancer cells

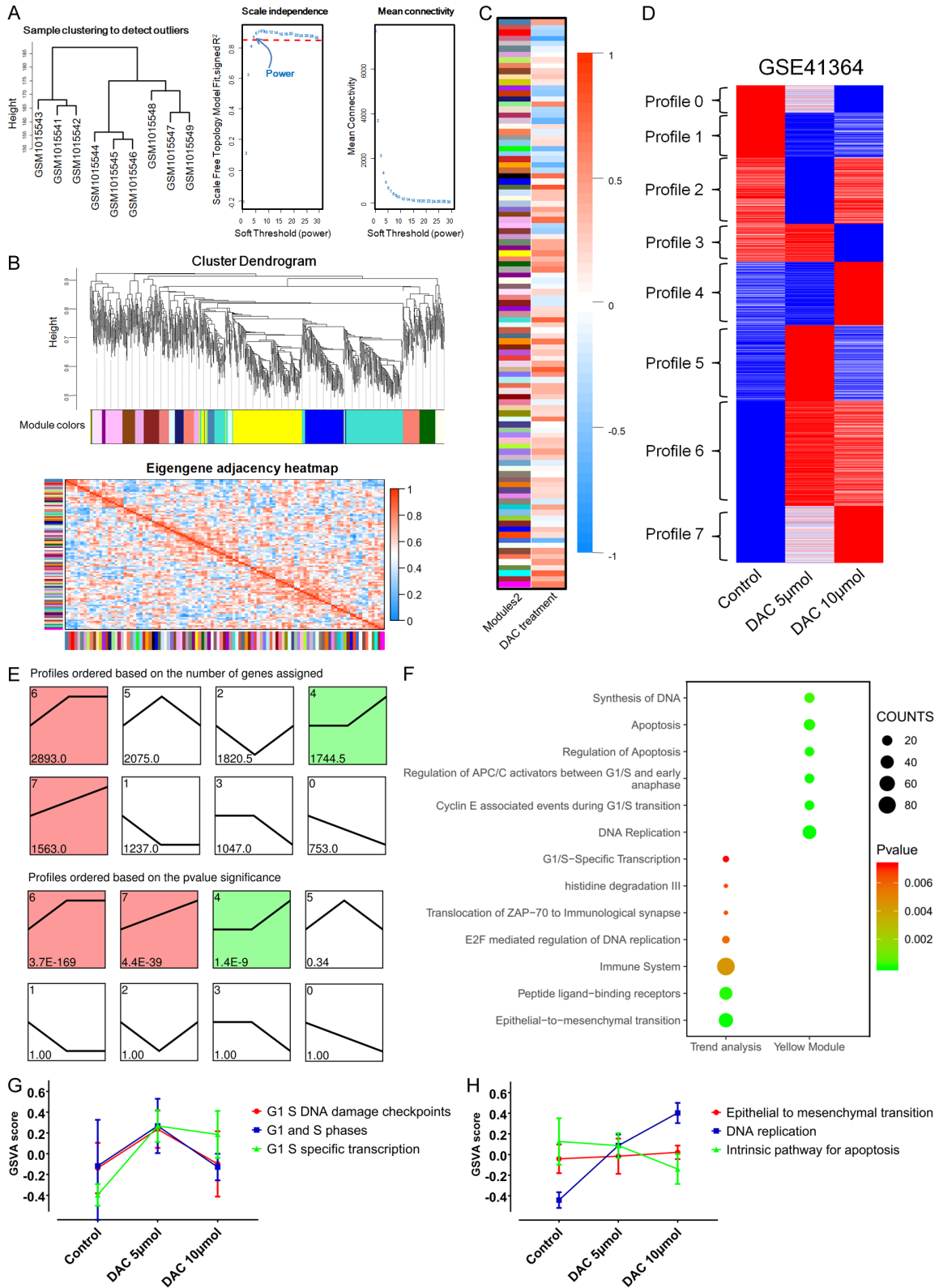


Figure 2. Weighted gene coexpression network analysis (WGCNA) and series test of cluster (STC) analysis. A. $\beta = 5$ was selected. B. A total of 103 modules were identified. C. A total of 6 modules was correlated with DAC treatment. D, E. STC analysis identified 3 profiles that contained genes with similar expression trends subject to DAC treatment, and profile 6 showed the highest significance ($P = 3.7E-169$). F. Pathway enrichment analysis of profile 6 and hub modules showed that DAC primarily modulated 3 pathways: G1/S-specific transcription involved in E2F-mediated regulation of Cyclin E-associated events, epithelial-to-mesenchymal transition (EMT) and regulation of apoptosis. G, H. GSVA showed the activity changes of these three pathways.

Low-dose decitabine treatment of HT29 colon cancer cells

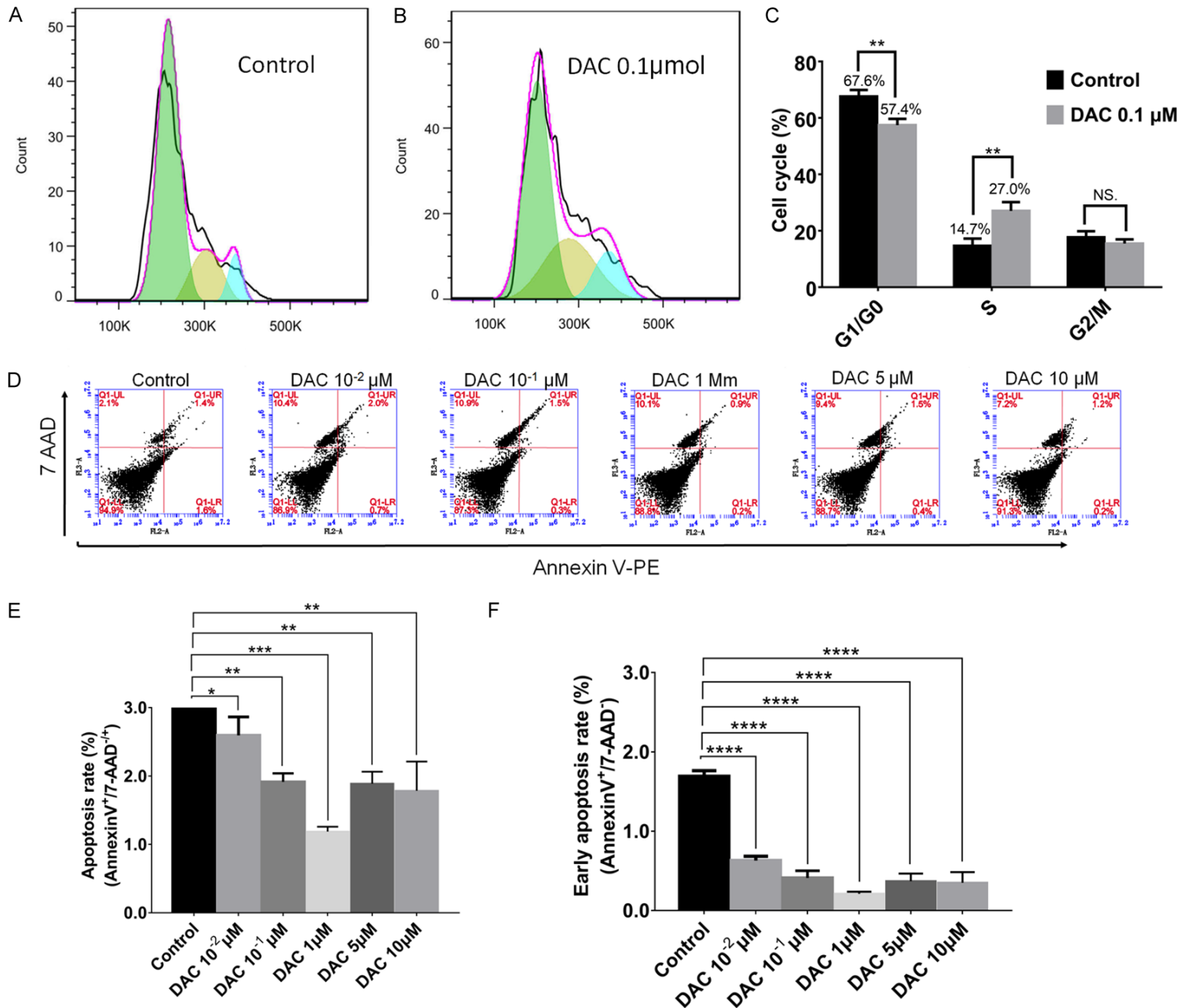


Figure 3. Low-dose DAC promoted G1/S-specific transcription and slightly decreased apoptosis in HT29 cells. A-C. Treatment with DAC at 0.1 μM resulted in an increase in cell numbers in the S phase relative to that in the control group (27.0% vs 14.7%) at the expense of G1 phase (57.4% vs 67.6%). D-F. The early apoptotic and total apoptotic cell rates decreased by ~1% when cells were coincubated with DAC at concentrations ranging from 10^{-2} to 10 μM .

markers Cyclin E1 and PCNA by western blotting (**Figure 5A**).

Verification of hub gene expression in the apoptotic pathway

We observed that low-dose DAC treatment slightly decreased the number of apoptotic cells. Moreover, BCL2, PCNA and FOXC1 were upregulated in DAC-treated HT-29 cells compared to controls in the GSE41364, GSE22598 and GSE32323 datasets (**Figure 4A, 4B**). To measure mRNA levels, qPCR assays were performed. After 48 h of incubation with 0.1 μM DAC, BCL2, PCNA and FOXC1 were upregulated compared with their levels in untreated HT-29 cells (**Figure 4D**). We also confirmed the expression of Bcl-2 protein by western blotting. Furthermore, western blot analysis showed that Bax protein levels were lower in DAC-treated cells than they were in controls (**Figure 5B**).

Verification of hub gene expression in the EMT pathway

By bioinformatic analysis, VIM, CXCL1 and VCAM1 were found to be upregulated in DAC-treated HT-29 cells compared to controls in the GSE41364, GSE22598 and GSE32323 datasets (**Figure 4A, 4B**). However, inconsistent results exist regarding the expression changes of CDH1 and SNAI2 subject to DAC treatment. Further qPCR assays demonstrated that the expression of VIM, CXCL1 and VCAM1 increased after 48 h of 0.1 μM DAC treatment (**Figure 4E**).

Analysis of promoter methylation of the DAC-activated gene BCL2 in CRC

Our abovementioned results confirmed that low-dose DAC activated G1/S-specific transcription and decreased apoptosis. Furthermore, low-dose DAC treatment increased the expression of BCL2 at the mRNA and protein levels. The oncogene BCL2 is regarded as “the general suppressor of cell death”, and it is directly involved in the regulation of apoptosis [27]. However, the present analysis, which was

based on 499 colon cancer cases from the TCGA database, revealed that BCL2 mRNA expression was decreased in colon cancer compared with mucosa (14.4 ± 1.1 vs 16.3 ± 0.3 , $P < 0.0001$, **Figure 6A**). Further analysis of 19 GEO-sourced datasets from Oncomine confirmed a similar and robust result ($P = 2.27\text{E-}6$, **Figure 6B**). To discover the underlying upstream regulatory mechanism by which BCL2 levels decreased in CRC, we analyzed the promoter methylation of BCL2 in colon cancer patients from the TCGA database and found that BCL2 had an increased level of methylation at 12 methylated sites in the promoter region of colon cancer compared with that of normal colon tissues (**Figure 6C**).

DNA promoter methylation level of BCL2 in HT-29 cells subjected to low-dose DAC treatment

A 2,000 bp sequence upstream of the transcription start site of BCL2 was considered the promoter region, and CpG islands within this region were predicted using the MethPrimer online platform. There was a CpG island located from -925 to 1857 in the promoter region of BCL2. The BSP primer targeting this CpG island is shown in **Figure 5C**. After low-dose DAC treatment, the DNA methylation rate of the BCL2 promoter region decreased relative to that of the control group (41.1% vs 57.9%, **Figure 5D**).

Discussion

The epigenetic drug DAC exhibits therapeutic efficiency for the treatment of several hematological malignancies [28]. However, clinical trials evaluating the efficacy of epigenetic drugs in the treatment of CRC failed to show an improvement in long-term survival [29]. In contrast, the present study revealed that a low-dose DAC of 0.1 μM promoted the proliferation and colony formation ability of HT-29 cells. Since demethylation across the whole genome changes the expression of a wide variety of genes, the effects of DAC in various tumor cells are hard to predict [30, 31]. Mapping all DAC-activated genes onto networks may elucidate key pathways activated after DAC treatment. Therefore, two system-level analytical tech-

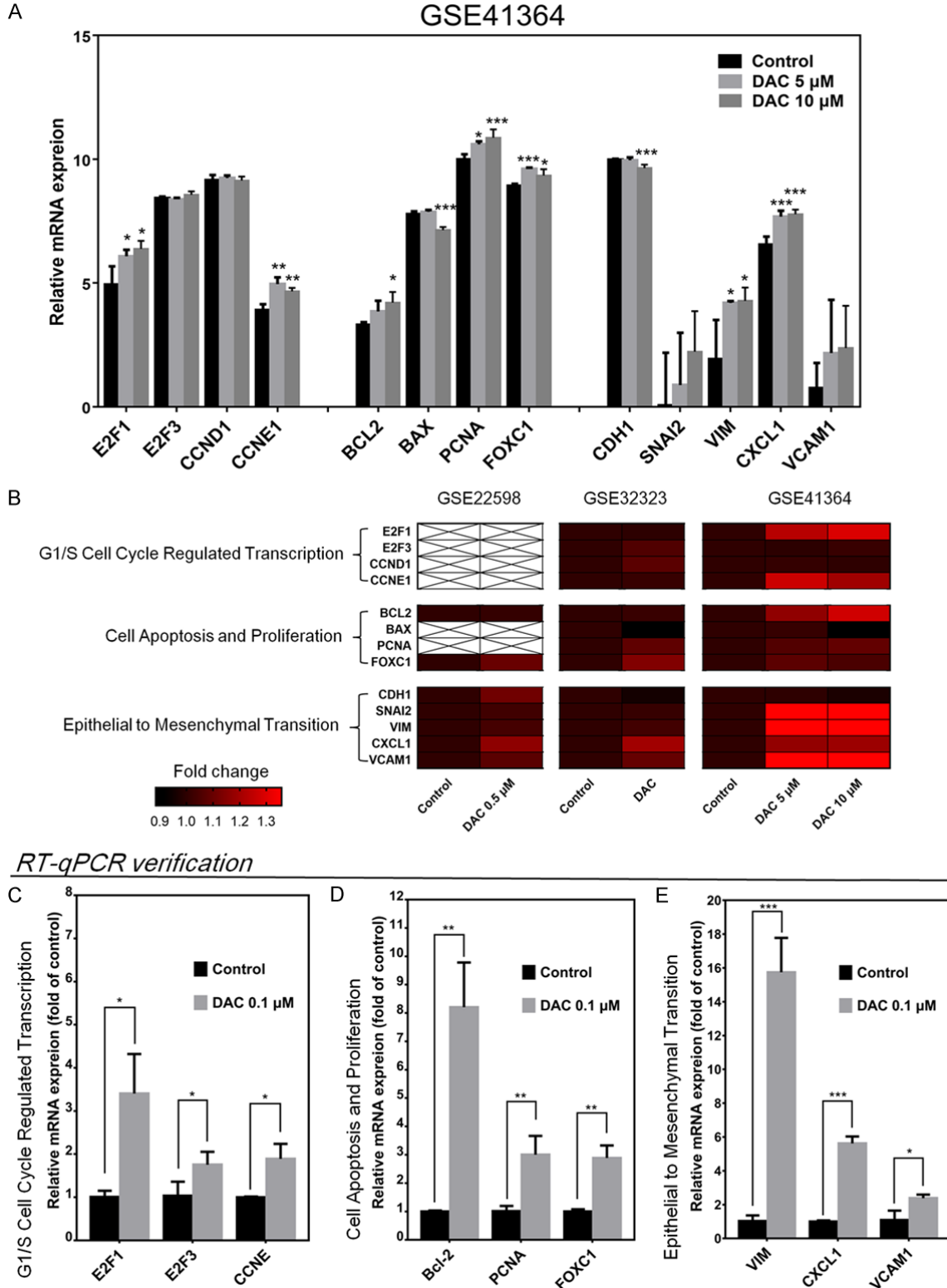


Figure 4. Verification of hub gene expression changes in 3 hub pathways at the mRNA level. (A, B) The regulatory hub oncogenes in these 3 pathways were upregulated after DAC treatment in three independent datasets of GSE41364, GSE32323 and GSE22598. RT-qPCR was performed in vitro. The regulatory hub oncogenes were confirmed to be activated by low-dose 0.1 μM DAC treatment in the (C) E2F/CCNE1 pathway, (D) apoptotic pathway, and (E) EMT pathway.

Low-dose decitabine treatment of HT29 colon cancer cells

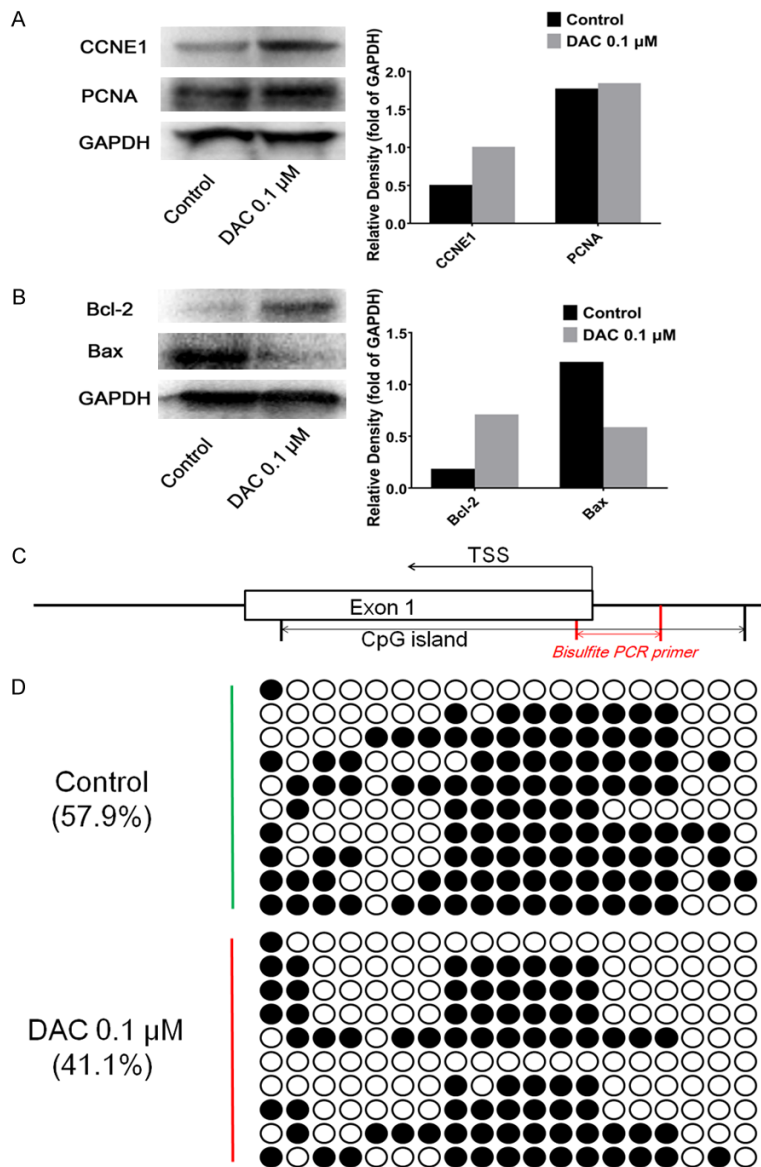


Figure 5. DNA promoter methylation level of BCL2 in HT-29 cells subjected to low-dose DAC treatment. Western blotting was performed. The protein expression of (A) Cyclin E1, PCNA and (B) Bcl-2 increased after 0.1 μ M DAC treatment. (C) There was a CpG island located from -925 to 1857 in the promoter region of BCL2. The red line indicates the BSP primer targeting this CpG island. (D) BSP showed that the DNA methylation rate at the BCL2 promoter region decreased in the DAC-treated group compared to that in the control group (41.1% vs 57.9%). TSS: transcription start site; BSP, bisulfite sequencing PCR.

niques, STC and WGCNA, were employed to identify network-central genes associated with DAC treatment. The system-level analysis showed that DAC modulated 3 critical pathways, G1/S-specific transcription involved in E2F-mediated regulation of Cyclin E-associated events, the apoptosis pathway and the EMT pathway. Further GSEA showed that G1/S-

specific transcription was activated by a low-dose DAC treatment and was inhibited at a higher dose. Subsequently, the promotion of G1/S phase-specific transcription was confirmed by flow cytometry analysis, as 0.1 μ M DAC resulted in an increase in cells in the S phase at the expense of G1 phase. The percentage of cells in S phase is known to be an index of cell proliferation [32]. In studies by Xiong et al. [33], DAC was shown to inhibit HT29 by blocking cells in the G2 phase. However, the concentration of DAC of 5 μ M in that study exceeded the tolerance dose accepted for humans of less than 0.3 μ M. Similarly, the present study also revealed an inhibitory effect of DAC in HT29 cells at concentrations larger than 10 μ M, which was a result of cytotoxicity rather than DNA demethylation [33]. Regarding the mechanism for promoting G1/S-specific gene transcription, low-dose DAC treatment increased E2F1 and CCNE1 expression. E2F1, which encodes the G1/S phase-specific transcription factor, was upregulated and positively correlated with the malignant phenotypes of CRC [34]. Cyclin E (CCNE), involved in the E2F/CCNE1 pathway [35], is another well-known oncogene [36]. In addition, apoptosis was inhibited after DAC treatment in the initial GSEA analysis. In our further in vitro experiments, the percentage of early apoptotic

and total apoptotic cells slightly decreased when cells were cocultured with low-dose DAC. Mechanistically, three oncogenes, BCL2, PCNA and FOXC1, were upregulated after low-dose DAC treatment. PCNA plays an important role in determining the fate of the replication fork and tumor development [37]. FOXC1 has been highlighted as a central transcription fac-

Low-dose decitabine treatment of HT29 colon cancer cells

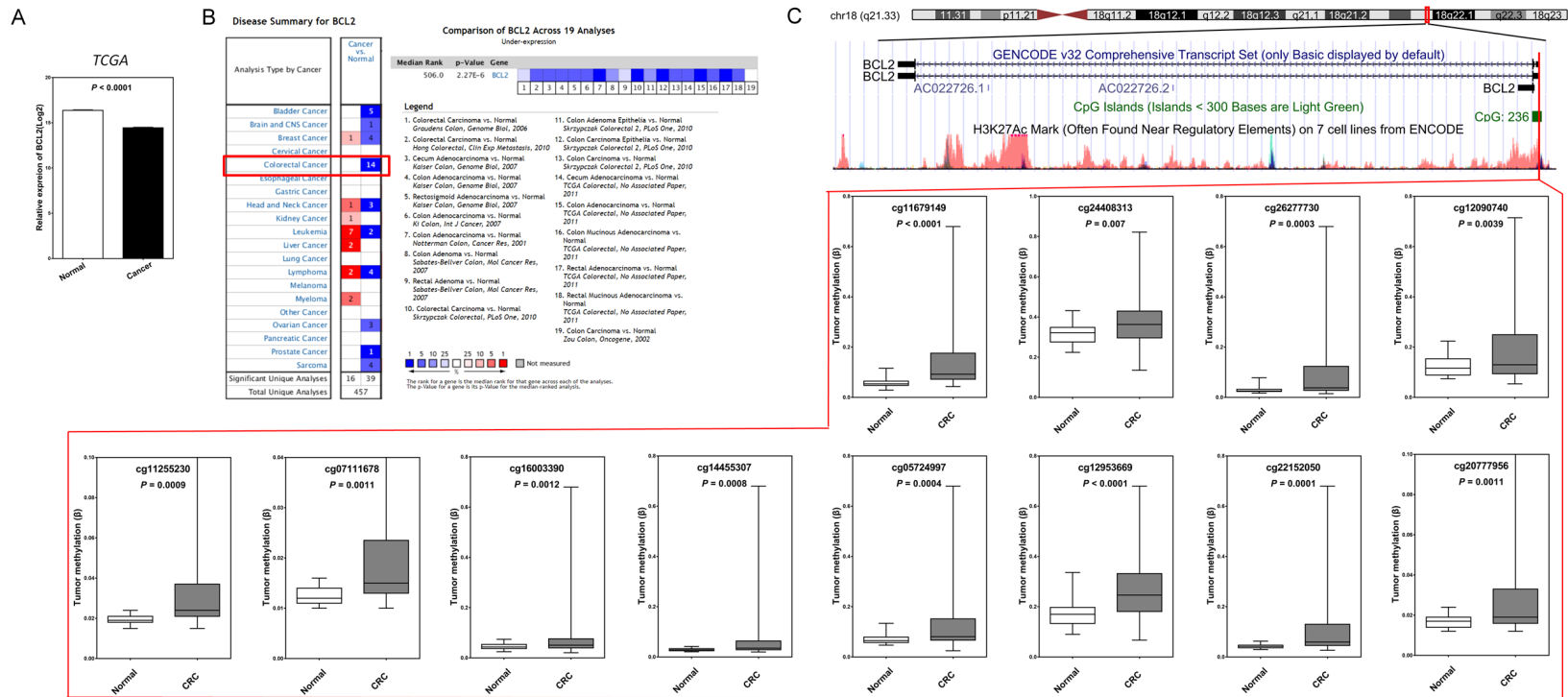


Figure 6. Analysis of promoter methylation of the DAC-activated gene BCL2 in CRC. A. BCL2 mRNA expression was decreased in colon cancer compared with that of normal mucosa in colon cancer patients from TCGA database (14.4 ± 1.1 vs 16.3 ± 0.3 , $P < 0.0001$). B. Analysis of the OncoPrint database confirmed that BCL2 mRNA expression was downregulated in CRC patients in 19 datasets ($P = 2.27E-6$). C. BCL2 had an increased degree of methylation in 12 methylated sites in the promoter region of colon cancer compared with normal colon tissues based on analysis of the TCGA database.

tor for tumor-associated genes [38], and its increase is associated with poor prognosis in many cancers [39]. In brief, the above results indicated that low-dose DAC promoted HT29 proliferation, enhanced G1/S phase transcription and decreased apoptosis through activation of several hub oncogenes.

DAC inhibits the EMT phenotype of a wide variety of tumor cell types [40, 41], including several types of CRC cells [42]. EMT, wherein epithelial cells depolarize, lose their cell-cell contacts, and gain an elongated, fibroblast-like morphology, is a typical initial process by which tumor cells gain cell-invasive behavior [43]. In contrast, in this study, parental HT-29 cells exhibited a cobblestone shape, while 0.1 μM DAC-treated HT-29 cells exhibited a spindle shape with mesenchymal morphology. Mechanistically, VIM, CXCL1 and VCAM1 were upregulated in DAC-treated HT-29 cells. Up-regulation of VIM, a marker for EMT [44], and VCAM-1 contributes to the poor prognosis of CRC [45, 46]. CXCL1 is crucial to the formation of a premetastatic niche and metastasis in CRC [47]. Demethylation treatment was also reported to cause the acquisition of mesenchymal characteristics in several well-defined gastric and prostate cancer cells [48, 49]. However, due to the inability of HT-29 cells to tolerate serum-free medium (data not shown), we did not perform scratch adhesion tests and cell invasion assays.

One hypothesis regarding the conflicting results between the effects of DAC on different cancer cell lines is that the pleiotropic effect of DAC is based on the combined activation of many genes that might have opposing roles. Whether the dominant effect of DAC on cancer is in promoting or suppressing is dependent on the balance between the activation of tumor suppressor genes and oncogenes. In this work, by employing system-level analytical techniques, we identified the key activated pathways involving several hub oncogenes activated by DAC in the HT29 cell line model. We chose the oncogene BCL2 as an example to determine the effect of low-dose DAC on BCL2 expression and methylation status. BCL2 has an increased promoter methylation level and decreased expression in colon cancer compared with normal mucosa. This indicated that high methylation at the promoter region of BCL2 plays a role in suppressing CRC by inhibiting the expression of

BCL2. However, after low-dose DAC treatment, the degree of DNA methylation at the BCL2 promoter region decreased, whereas its expression increased, which blocks the apoptotic death of HT-29 cells. A similar mechanism has been reported in a noncancer cell model of human umbilical vascular endothelial cells. The epigenetic modification, demethylation of the Bcl-2 promoter, alleviated endothelial apoptosis by increasing Bcl-2 expression [50].

There were inadequacies in the present study. We used only one CRC cell line, HT29. Previous studies showed that a low dose of 2-2.5 μM DAC inhibited the growth of SW620 and HCT116 CRC cells [51]. Another study showed that a dose of 10 μM had no effect on the apoptosis rate of HT29 but significantly induced apoptosis of COLO205 and SW620 CRC cells [52]. HCT116 CRC cells have the highest sensitivity, while HT29 CRC cells exhibit the highest resistance to DAC [12]. The effect of low-dose DAC treatment on various CRC cell lines needs to be directly compared in our future research. In addition, the genetic background of HT29 was not analyzed in the present study. Further analysis of the genetic background of the HT29 cell line, such as determination BRAF mutation status [53], may shed light on understanding the mechanism of intrinsic DAC resistance. Considering CRC interindividual heterogeneity, identifying molecular subtypes of CRC by a system-level technique might determine how and whether patients will benefit from DAC treatments [54].

In conclusion, low-dose DAC promotes the proliferation and colony formation ability of HT-29 cell lines. The results of the system-level analysis with STC, WGCNA and GSEA showed that DAC modulated 3 critical pathways: E2F-mediated G1/S-specific transcription, the apoptosis pathway and the EMT pathway. The effect of DAC on phenotypes was subsequently confirmed. Several regulatory hub oncogenes in these 3 pathways, CCNE1, E2F1, BCL2, PCNA, FOXC1, VIM, CXCL1 and VCAM1, were further confirmed to be activated by DAC at either the mRNA or protein level in our in vitro experiments. Mechanistically, high methylation at the promoter region of oncogenes with dominant effects in CRC, such as what is observed in BCL2 in HT29 cells, might play a role in suppressing CRC by inhibiting its expression. Low-dose DAC triggers its expression by decreasing

its promoter methylation level, thereby resulting in cancer promotion. To refine DAC treatment, molecular subtypes of CRC might need to be considered to predict which tumors will benefit from epigenetic treatments, which needs further study.

Acknowledgements

This study was financially supported by National Clinical Key Specialty Construction Project (General Surgery) of China (No. 2012-649), National Natural Science Foundation of China (81902378), Joint Funds for the Innovation of Science and Technology, Fujian province (2017Y9104).

Disclosure of conflict of interest

None.

Address correspondence to: Dr. Pan Chi, Department of Colorectal Surgery, Union Hospital, Fujian Medical University, 29 Xin-Quan Road, Fuzhou 350001, Fujian, People's Republic of China. Tel: +86-13675089677; Fax: +86-0591-87113828; E-mail: chipan363@163.com

References

[1] Vuik FE, Nieuwenburg SA, Bardou M, Lansdorp-Vogelaar I, Dinis-Ribeiro M, Bento MJ, Zadnik V, Pellisé M, Esteban L, Kaminski MF, Suchanek S, Ngo O, Májek O, Leja M, Kuipers EJ and Spaander MC. Increasing incidence of colorectal cancer in young adults in Europe over the last 25 years. *Gut* 2019; 68: 1820-1826.

[2] Huiskens J, van Gulik TM, van Lienden KP, Engelbrecht MRW, Meijer GA, van Grieken NCT, Schriek J, Keijser A, Mol L, Molenaar Q, Verhoef C, de Jong KP, Dejong KHC, Kazemier G, Ruers TM, de Wilt JHW, van Tinteren H and Punt CJA. Treatment strategies in colorectal cancer patients with initially unresectable liver-only metastases, a study protocol of the randomised phase 3 CAIRO5 study of the dutch colorectal cancer group (DCCG). *BMC Cancer* 2015; 15: 365.

[3] Zheng R, Gao D, He T, Zhang M, Zhang X, Linghu E, Wei L and Guo M. DIRAS1 methylation of promotes colorectal cancer progression and may serve as a marker for poor prognosis. *Clin Epigenetics* 2017; 9: 50.

[4] Pogribny IP and Beland FA. DNA methylome alterations in chemical carcinogenesis. *Cancer Lett* 2013; 334: 39-45.

[5] Azad N, Zahnow CA, Rudin CM and Baylin SB. The future of epigenetic therapy in solid tu-

mours—lessons from the past. *Nat Rev Clin Oncol* 2013; 10: 256-266.

[6] Faraoni I, Consalvo MI, Aloisio F, Fabiani E, Giansanti M, Cristino FD, Falconi G, Tentori L, Veroli AD, Curzi P, Maurillo L, Niscola P, Lo-Coco F, Graziani G and Voso MT. Cytotoxicity and differentiating effect of the poly(ADP-Ribose) polymerase inhibitor olaparib in myelodysplastic syndromes. *Cancers* 2019; 11: 1373.

[7] Müller MF, Ibrahim A and Arends MJ. Molecular pathological classification of colorectal cancer. *Virchows Arch* 2016; 469: 125-134.

[8] Patnaik S and Anupriya. Drugs targeting epigenetic modifications and plausible therapeutic strategies against colorectal cancer. *Front Pharmacol* 2019; 10: 588.

[9] Ross JS, Fakhri M, Ali SM, Elvin JA, Schrock AB, Suh J, Vergilio J, Ramkissoon S, Severson E, Daniel S, Fabrizio D, Frampton G, Sun J, Miller VA, Stephens PJ and Gay LM. Targeting HER2 in colorectal cancer: the landscape of amplification and short variant mutations in ERBB2 and ERBB3. *Cancer* 2018; 124: 1358-1373.

[10] Ali Hassan NZ, Mokhtar NM, Sin TK, Rose IM, Sagap I, Harun R and Jamal R. Integrated analysis of copy number variation and genome-wide expression profiling in colorectal cancer tissues. *PLoS One* 2014; 9: e92553.

[11] Qu X, Sandmann T, Frierson H Jr, Fu L, Fuentes E, Walter K, Okrah K, Rumpel C, Moskaluk C, Lu S, Wang Y, Bourgon R, Penuel E, Pirzkal A, Amler L, Lackner MR, Taberero J, Hampton GM and Kabbarah O. Integrated genomic analysis of colorectal cancer progression reveals activation of EGFR through demethylation of the EREG promoter. *Oncogene* 2016; 35: 6403-6415.

[12] Ikehata M, Ogawa M, Yamada Y, Tanaka S, Ueda K and Iwakawa S. Different effects of epigenetic modifiers on the cytotoxicity induced by 5-fluorouracil, irinotecan or oxaliplatin in colon cancer cells. *Biol Pharm Bull* 2014; 37: 67-73.

[13] Flis S, Gnyszka A and Flis K. DNA methyltransferase inhibitors improve the effect of chemotherapeutic agents in SW48 and HT-29 colorectal cancer cells. *PLoS One* 2014; 9: e92305.

[14] Cashen AF, Shah AK, Todt L, Fisher N and DiPersio J. Pharmacokinetics of decitabine administered as a 3-h infusion to patients with acute myeloid leukemia (AML) or myelodysplastic syndrome (MDS). *Cancer Chemother Pharmacol* 2008; 61: 759-766.

[15] Luan S, Li P and Yi T. Series test of cluster and network analysis for lupus nephritis, before and after IFN-K-immunosuppressive therapy. *Nephrology (Carlton)* 2018; 23: 997-1006.

Low-dose decitabine treatment of HT29 colon cancer cells

- [16] Wang X, Ghareed WM, Zhang Y, Yu Q, Lu X, Huang Y, Huang S, Sun Y and Chi P. Hypermethylated and downregulated MEIS2 are involved in stemness properties and oxaliplatin-based chemotherapy resistance of colorectal cancer. *J Cell Physiol* 2019; 234: 18180-18191.
- [17] Xu X, Zhang Y, Williams J, Antoniou E, McCombie WR, Wu S, Zhu W, Davidson NO, Denoya P and Li E. Parallel comparison of illumina RNA-Seq and affymetrix microarray platforms on transcriptomic profiles generated from 5-aza-deoxy-cytidine treated HT-29 colon cancer cells and simulated datasets. *BMC Bioinformatics* 2013; 14 Suppl 9: S1.
- [18] Khamas A, Ishikawa T, Shimokawa K, Mogushi K, Iida S, Ishiguro M, Mizushima H, Tanaka H, Uetake H and Sugihara K. Screening for epigenetically masked genes in colorectal cancer Using 5-Aza-2'-deoxycytidine, microarray and gene expression profile. *Cancer Genomics Proteomics* 2012; 9: 67-75.
- [19] Okazaki S, Ishikawa T, Iida S, Ishiguro M, Kobayashi H, Higuchi T, Enomoto M, Mogushi K, Mizushima H, Tanaka H, Uetake H and Sugihara K. Clinical significance of UNC5B expression in colorectal cancer. *Int J Oncol* 2012; 40: 209-216.
- [20] Koch A, Meyer TD, Jeschke J and Crieckinge WV. MEXPRESS: visualizing expression, DNA methylation and clinical TCGA data. *BMC Genomics* 2015; 16: 636.
- [21] Rhodes DR, Yu J, Shanker K, Deshpande N, Varambally R, Ghosh D, Barrette T, Pandey A and Chinnaiyan AM. ONCOMINE: a cancer microarray database and integrated data-mining platform. *Neoplasia* 2004; 6: 1-6.
- [22] Botía JA, Vandrovcova J, Forabosco P, Guelfi S, D'Sa K; United Kingdom Brain Expression Consortium, Lewis CM, Ryten M and Weale ME. An additional k-means clustering step improves the biological features of WGCNA gene co-expression networks. *BMC Syst Biol* 2017; 11: 47.
- [23] Ravasz E, Somera AL, Mongru DA, Oltvai ZN and Barabási AL. Hierarchical organization of modularity in metabolic networks. *Science* 2002; 297: 1551-1555.
- [24] Pathan M, Keerthikumar S, Chisanga D, Alessandro R, Ang C, Askenase P, Batagov AO, Benito-Martin A, Camussi G, Clayton A, Collino F, Vizio DD, Falcon-Perez JM, Fonseca P, Fonseka P, Fontana S, Gho YS, Hendrix A, Hoen EN, Iraci N, Kastaniegaard K, Liang Y, Llorente A, Lunavat TR, Maji S, Monteleone F, Øverbye A, Panaretakis T, Patel T, Peinado H, Pluchino S, Principe S, Ronquist G, Royo F, Sahoo S, Spinelli C, Stensballe A, Théry C, van Herwijnen MJC, Wauben M, Welton JL, Zhao K and Mathivanan S. A novel community driven software for functional enrichment analysis of extracellular vesicles data. *J Extracell Vesicles* 2017; 6: 1321455.
- [25] Hänzelmann S, Castelo R and Guinney J. GSEA: gene set variation analysis for microarray and RNA-seq data. *BMC Bioinformatics* 2013; 14: 7.
- [26] Kim B, Shin H, Heo Y, Ha S, Jang K, Kim S, Kang W, Lee J and Kim K. CCNE1 amplification is associated with liver metastasis in gastric carcinoma. *Pathol Res Pract* 2019; 215: 152434.
- [27] Stoian M, State N, Stoica V and Radulian G. Apoptosis in colorectal cancer. *J Med Life* 2014; 7: 160-164.
- [28] Baretta M and Azad NS. The role of epigenetic therapies in colorectal cancer. *Curr Probl Cancer* 2018; 42: 530-547.
- [29] Vincent A, Ouelkdite-Oumouchal A, Souidi M, Leclerc J, Neve B and Seuningen IV. Colon cancer stemness as a reversible epigenetic state: implications for anticancer therapies. *World J Stem Cells* 2019; 11: 920-936.
- [30] Jiao F, Bai S, Ma Y, Yan Z, Yue Z, Yu Y, Wang X and Wang J. DNA methylation of heparanase promoter influences its expression and associated with the progression of human breast cancer. *PLoS One* 2014; 9: e92190.
- [31] Borge S, Döppler HR and Storz P. A combination treatment with DNA methyltransferase inhibitors and suramin decreases invasiveness of breast cancer cells. *Breast Cancer Res Treat* 2014; 144: 79-91.
- [32] Hedley DW, Rugg CA and Gelber RD. Association of DNA index and S-phase fraction with prognosis of nodes positive early breast cancer. *Cancer Res* 1987; 47: 4729-4735.
- [33] Xiong H, Chen Z, Liang Q, Du W, Chen H, Su W, Chen G, Han Z and Fang J. Inhibition of DNA methyltransferase induces G2 cell cycle arrest and apoptosis in human colorectal cancer cells via inhibition of JAK2/STAT3/STAT5 signalling. *J Cell Mol Med* 2009; 13: 3668-3679.
- [34] Fang Z, Gong C, Liu H, Zhan X, Mei L, Song M, Qiu L, Luo S, Zhu Z, Zhang R, Gu H and Chen X. E2F1 promote the aggressiveness of human colorectal cancer by activating the ribonucleotide reductase small subunit M2. *Biochem Biophys Res Commun* 2015; 464: 407-415.
- [35] Wang F, Mao A, Tang J, Zhang Q, Yan J, Wang Y, Di C, Gan L, Sun C and Zhang H. microRNA-16-5p enhances radiosensitivity through modulating Cyclin D1/E1-pRb-E2F1 pathway in prostate cancer cells. *J Cell Physiol* 2019; 234: 13182-13190.
- [36] Li W, Zhang G, Wang H and Wang L. Analysis of expression of cyclin E, p27kip1 and Ki67 protein in colorectal cancer tissues and its value for diagnosis, treatment and prognosis of dis-

Low-dose decitabine treatment of HT29 colon cancer cells

- ease. *Eur Rev Med Pharmacol Sci* 2016; 20: 4874-4879.
- [37] Stoimenov I and Helleday T. PCNA on the cross-road of cancer. *Biochem Soc Trans* 2009; 37: 605-613.
- [38] Yang Z, Jiang S, Cheng Y, Li T, Hu W, Ma Z, Chen F and Yang Y. FOXC1 in cancer development and therapy: deciphering its emerging and divergent roles. *Ther Adv Med Oncol* 2017; 9: 797-816.
- [39] Han B, Bhowmick N, Qu Y, Chung S, Giuliano AE and Cui X. FOXC1: an emerging marker and therapeutic target for cancer. *Oncogene* 2017; 36: 3957-3963.
- [40] Wang X, Wang J, Jia Y, Wang Y, Han X, Duan Y, Lv W, Ma M and Liu L. Methylation decreases the Bin1 tumor suppressor in ESCC and restoration by decitabine inhibits the epithelial mesenchymal transition. *Oncotarget* 2017; 8: 19661-19673.
- [41] Zhang N, Liu Y, Wang Y, Zhao M, Tu L and Luo F. Decitabine reverses TGF- β 1-induced epithelial-mesenchymal transition in non-small-cell lung cancer by regulating miR-200/ZEB axis. *Drug Des Devel Ther* 2017; 11: 969-983.
- [42] Tanaka S, Hosokawa M, Ueda K and Iwakawa S. Effects of decitabine on invasion and exosomal expression of miR-200c and miR-141 in oxaliplatin-resistant colorectal cancer cells. *Biol Pharm Bull* 2015; 38: 1272-1279.
- [43] Fischer KR, Durrans A, Lee S, Sheng J, Li F, Wong STC, Choi H, Rayes TE, Ryu S, Troeger J, Schwabe RF, Vahdat LT, Altorki NK, Mittal V and Gao D. Epithelial-to-mesenchymal transition is not required for lung metastasis but contributes to chemoresistance. *Nature* 2015; 527: 472-476.
- [44] Satelli A and Li S. Vimentin in cancer and its potential as a molecular target for cancer therapy. *Cell Mol Life Sci* 2011; 68: 3033-3046.
- [45] Du L, Li J, Lei L, He H, Chen E Dong J and Yang J. High vimentin expression predicts a poor prognosis and progression in colorectal cancer: a study with meta-analysis and TCGA database. *Biomed Res Int* 2018; 2018: 6387810.
- [46] Dymicka-Piekarska V, Guzinska-Ustymowicz K, Kuklinski A and Kemonia H. Prognostic significance of adhesion molecules (sICAM-1, sV-CAM-1) and VEGF in colorectal cancer patients. *Thromb Res* 2012; 129: e47-50.
- [47] Wang D, Sun H, Wei J, Cen B and DuBois RN. CXCL1 is critical for premetastatic niche formation and metastasis in colorectal cancer. *Cancer Res* 2017; 77: 3655-3665.
- [48] Li D, Xu C, Cui R, Tang J, Sun H, Yang Z, Bu J, Lin P, Huang N, Du Y and Yu X. DNA methylation inhibitor, decitabine, promotes MGC803 gastric cancer cell migration and invasion via the upregulation of NEDD4-1. *Mol Med Rep* 2015; 12: 8201-8208.
- [49] Dudzik P, Trojan SE, Ostrowska B, Zemanek G, Dulińska-Litewka J, Laidler P and Kocemba-Pilarczyk KA. CD146 the epigenetic modifier 5-Aza-2-deoxycytidine triggers the expression of gene in prostate cancer cells. *Anticancer Res* 2019; 39: 2395-2403.
- [50] Zeng H, Kong X, Zhang H, Chen Y, Cai S, Luo H and Chen P. Inhibiting DNA methylation alleviates cigarette smoke extract-induced dysregulation of Bcl-2 and endothelial apoptosis. *Tob Induc Dis* 2020; 18: 51.
- [51] Li S, Han Z, Zhao N, Zhu B, Zhang Q, Yang X, Sheng D, Hou J, Guo S, Wei L and Zhang L. Inhibition of DNMT suppresses the stemness of colorectal cancer cells through down-regulating Wnt signaling pathway. *Cell Signal* 2018; 47: 79-87.
- [52] Lin J, Lai M, Huang Q, Ruan W, Ma Y and Cui J. Reactivation of IGFBP7 by DNA demethylation inhibits human colon cancer cell growth in vitro. *Cancer Biol Ther* 2008; 7: 1896-1900.
- [53] Zhang P, Kawakami H, Liu W, Zeng X, Strebhardt K, Tao K, Huang S and Sinicrope FA. Targeting CDK1 and MEK/ERK overcomes apoptotic resistance in BRAF-mutant human colorectal cancer. *Mol Cancer Res* 2018; 16: 378-389.
- [54] Garrido-Laguna I, McGregor KA, Wade M, Weis J, Gilcrease W, Burr L, Soldi R, Jakubowski L, Davidson C, Morrell G, Olpin JD, Boucher K, Jones D and Sharma S. A phase I/II study of decitabine in combination with panitumumab in patients with wild-type (wt) KRAS metastatic colorectal cancer. *Invest New Drugs* 2013; 31: 1257-1264.